Eur. Phys. J. B **16**, 537–541 (2000)

THE EUROPEAN PHYSICAL JOURNAL B

EDP Sciences

Globally coupled systems with prescribed synchronized dynamics

D.H. Zanette[a,b]

Centro Atómico Bariloche and Instituto Balseiro, 8400 Bariloche, Río Negro, Argentina

Received 22 October 1999

Abstract. A system of globally coupled maps whose synchronized dynamics differs from the individual (chaotic) evolution is considered. For nonchaotic synchronized dynamics, the synchronized state becomes stable at a critical coupling intensity lower than that of the fully chaotic case. Below such critical point, synchronization is also stable in a set of finite intervals. Moreover, the system is shown to exhibit multistability, so that even when the synchronized state is stable not all the initial conditions lead to synchronization of the ensemble.

PACS. 05.45.Xt Synchronization; coupled oscillators – 05.45.-a Nonlinear dynamics and nonlinear dynamical systems – 05.45.Pq Numerical simulations of chaotic models

Synchronization is a form of collective behavior frequently found in complex natural systems within the scopes of both physics and life sciences. This phenomenon has been observed in physico-chemical reactions [1], electronic circuits [2], neural systems [3], and social behavior [4], among other. Synchronized dynamics, which is characterized by the coherent evolution of the elements in an interacting ensemble, seems to be typical of systems with long-range interactions [5]. As a matter of fact, a standard model for synchronization in complex dynamical systems is given by a set of N globally coupled maps [6],

$$\mathbf{x}_i(t+1) = (1-\epsilon)\mathbf{f}[\mathbf{x}_i(t)] + \frac{\epsilon}{N}\sum_{j=1}^{N}\mathbf{f}[\mathbf{x}_j(t)] \qquad (1)$$

$(i = 1, \ldots, N)$, where the interaction does not depend at all on the distance between elements. Here, ϵ measures the strength of coupling ($0 \leq \epsilon \leq 1$), and $\mathbf{f}(\mathbf{x})$ defines the individual dynamics of each element. For $\epsilon = 0$ the elements evolve independently of each other. On the other hand, for $\epsilon = 1$ the system is fully synchronized after the first time step. All the elements collapse into a single point cluster. The synchronized state, where the orbits $\mathbf{x}_i(t)$ of all elements are identical, is stable when $(1-\epsilon)\exp\lambda < 1$, where λ is the largest Lyapunov exponent of the map defined by $\mathbf{f}(\mathbf{x})$. For a chaotic map ($\lambda > 0$) there exists a critical value of the coupling intensity, $0 < \epsilon_c < 1$, above which synchronization is stable [6]. For a nonchaotic map ($\lambda < 0$) the ensemble synchronizes for any $\epsilon > 0$.

In model (1), when the ensemble becomes synchronized the dynamics of the collapsed cluster reproduces exactly that of a single, independent element. However, in several real instances of synchronized behavior – notably, in pathological neurological states – synchronization is accompanied by a qualitative change in the global dynamics of the system. During epileptic episodes, in fact, the coherent activity of vast zones of the cerebral cortex is almost periodic, strongly contrasting with the seemingly chaotic patterns of normal brain function [7]. In insect societies, collective dynamics can be qualitatively different from individual motion [8]. Swarms evolve in a wide variety of forms which does not reflect diversity in the elementary behavior, but rather in the interaction between individuals. Finally, in the engineering of coupled automata designed to perform specific tasks, the expected ensemble evolution is typically more complex than the individual dynamics. It is therefore relevant to consider ensembles of coupled dynamical elements able to exhibit coherent behavior, but such that the synchronized dynamics differs from that of the individuals. In the following, a generalization of equation (1) with the above property is considered. For sufficiently strong coupling, the ensemble collapses to a synchronized state with prescribed evolution, which is in general different from the individual behavior. The transition between both regimes is studied and some significant differences with the usual model (1) are pointed out.

Consider the following set of globally coupled maps:

$$\mathbf{x}_i(t+1) = (1-\epsilon)\mathbf{f}_1[\mathbf{x}_i(t)] + \frac{\epsilon}{N}\sum_{j=1}^{N}\mathbf{f}_2[\mathbf{x}_j(t)] \qquad (2)$$

$(i = 1, \ldots, N)$. Here, as in equation (1), ϵ measures the strength of coupling. For $\epsilon = 0$ the evolution of each element is governed by its individual dynamics, which

[a] Also at Consejo Nacional de Investigaciones Científicas y Técnicas, Argentina. This work has partially been carried out at the Abdus Salam International Centre for Theoretical Physics, Trieste, Italy.

[b] e-mail: zanetted@ictp.trieste.it

is prescribed by the function $\mathbf{f}_1(\mathbf{x})$, *i.e.* $\mathbf{x}(t+1) = \mathbf{f}_1[\mathbf{x}(t)]$. For $\epsilon = 1$, instead, all the elements collapse at the first time step into a single point cluster, whose trajectory is governed by the function $\mathbf{f}_2(\mathbf{x})$, *i.e.* $\mathbf{x}(t+1) = \mathbf{f}_2[\mathbf{x}(t)]$. For intermediate values of the coupling intensity, as ϵ grows, it is expected that the ensemble dynamics gradually replaces the individual evolution. In particular, there should exist a value ϵ_0 of the coupling intensity such that for $\epsilon > \epsilon_0$ the synchronized state is stable.

It is clear from equation (2) that if for a given value of ϵ the system is synchronized, the evolution of the collapsed ensemble will be governed by the map

$$\mathbf{x}(t+1) = \mathbf{F}[\mathbf{x}(t)] = (1-\epsilon)\mathbf{f}_1[\mathbf{x}(t)] + \epsilon \mathbf{f}_2[\mathbf{x}(t)]. \quad (3)$$

It could be expected that the dynamics defined by this map is somehow intermediate between the dynamics defined by $\mathbf{f}_1$ and $\mathbf{f}_2$. However, since these two functions are in general nonlinear, the behavior of the map given by their linear combination can be qualitatively different from that of the single maps. A suitable illustration of this fact, which will be useful in what follows, is provided by the (one-dimensional) logistic map [9]. Taking $f_k(x) = r_k x(1-x)$ $(k = 1, 2)$, one has $F(x) = rx(1-x)$, *i.e.* a logistic map with a modified parameter $r = (1-\epsilon)r_1 + \epsilon r_2$. For given ϵ, r_1 and r_2 can be chosen in such a way that, for instance, f_1 and f_2 produce regular evolution but F produces chaotic dynamics, or *vice versa*.

The onset of synchronization can be readily studied from linearization of equation (2) around the orbits of map (3). It turns out that the condition for stability of the synchronized state can be written as

$$(1-\epsilon)\exp \Lambda < 1. \quad (4)$$

Here, Λ is the largest Lyapunov exponent of the map defined by $\mathbf{f}_1(\mathbf{x})$, but *calculated along the orbit given by map* (3). For instance, for one-dimensional maps, Λ is be given by [9]

$$\Lambda = \lim_{T\to\infty} \frac{1}{T} \sum_{t=0}^{T} \ln |f_1'[x(t)]|\,, \quad (5)$$

with $x(t+1) = (1-\epsilon)f_1[x(t)] + \epsilon f_2[x(t)]$. The value of Λ results thus from a sampling of the Jacobian of $\mathbf{f}_1$ along the orbits of $\mathbf{F}$. If $\mathbf{f}_1$ defines a nonchaotic map, it is most likely that Λ will be negative, and equation (4) will be satisfied for any $\epsilon > 0$. As confirmed by numerical simulations, the ensemble becomes synchronized for arbitrarily small coupling intensities. Therefore, the specific cases considered below correspond to chaotic individual dynamics.

It is clear from equation (5) that Λ depends on ϵ, generally, in a complicated manner. Thus, the critical coupling intensity ϵ_c at which synchronization becomes stable is in general a complex function of Λ and can only be given implicitly, as

$$\epsilon_c = 1 - \exp[-\Lambda(\epsilon_c)]. \quad (6)$$

As shown numerically in the following example, this implicit equation can have many roots.

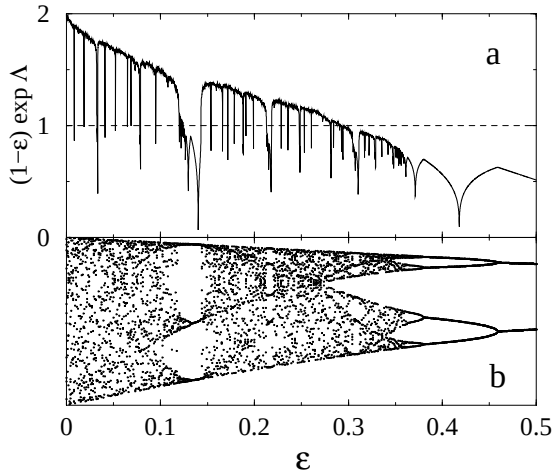

Fig. 1. (a) Numerical measurement of the quantity $(1-\epsilon)\exp \Lambda$ defined in equation (4) as a function of ϵ, for the case $f_1(x) = r_1 x(1-x)$ and $f_2(x) = r_2 x(1-x)$ with $r_1 = 4$ and $r_2 = 2.8$. (b) Bifurcation diagram of $F(x) = (1-\epsilon)f_1(x) + \epsilon f_2(x)$.

Figure 1a shows numerical measurements of the quantity $(1-\epsilon)\exp \Lambda(\epsilon)$ as a function of the coupling intensity for the case of two logistic maps quoted above, with $r_1 = 4$ [10] and $r_2 = 2.8$. For these values of the parameters the individual dynamics ($\epsilon = 0$) is chaotic whereas the fully coupled dynamics ($\epsilon = 1$) has a fixed point at $x \approx 0.64$. According to equation (4), for the values of ϵ where the graph is below the dashed horizontal line the state of full synchronization is linearly stable. In the present example, for small values of the coupling intensity ($\epsilon \lesssim 0.3$), this occurs in an irregular series of intervals. Figure 1b, where the bifurcation diagram of the map $F(x)$ has been plotted, reveals that these intervals correspond to the periodicity windows of the synchronized dynamics. Within these intervals, thus, the (stable) collapsed ensemble evolves along a periodic orbit. The well-known structure of periodicity windows in the logistic map suggests that such intervals could be infinitely many in number.

For $\epsilon > \epsilon_0 \approx 0.292$, the quantity $(1-\epsilon)\exp \Lambda(\epsilon)$ is always less than unity and the synchronized state is linearly stable. Note however that near ϵ_0 the dynamics of the collapsed ensemble can still be chaotic. In fact, $F(x)$ does not reach a definitive regime of periodic behavior up to $\epsilon \approx 0.35$. The coupling intensity ϵ_0 at which the synchronized state becomes definitively stable is to be compared with the corresponding critical coupling intensity of system (1). With $f(x) = f_1(x)$, synchronization is stable for $\epsilon > 0.5$. Meanwhile, for $f(x) = f_2(x)$ the synchronized state is stable for any $\epsilon > 0$, because the individual dynamics is nonchaotic. Therefore, the combination of the chaotic individual dynamics given by f_1 with the regular ensemble dynamics given by f_2 produces a sensible lowering of the critical point at which synchronization becomes stable. The appearance of stability windows as described above is an additional byproduct of this combination, not present in the usual case, equation (1).

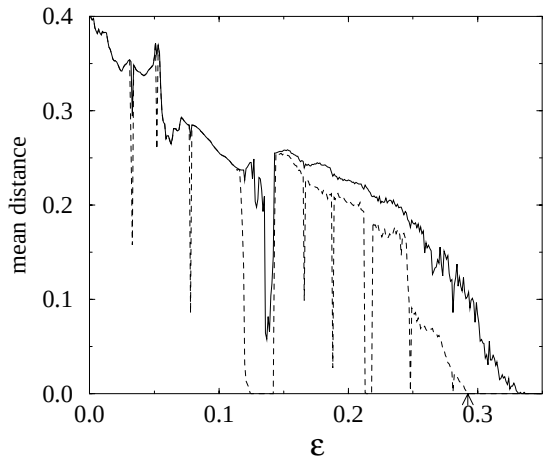

Fig. 2. Synchronization frequency Ω of the asymptotic modes $m = 0, \ldots, 3$ in a one-dimensional ensemble of $N = 100$ globally coupled oscillators with periodic boundary conditions, as a function of the nearest-neighbour delay time τ_0.

A possible candidate to play the role of an order parameter in the transition to synchronization is the mean distance between the elements in the ensemble [11],

$$d = \left\langle \frac{2}{N(N-1)} \sum_i \sum_{j<i} |\mathbf{x}_i(t) - \mathbf{x}_j(t)| \right\rangle , \qquad (7)$$

where $|\cdot|$ is a suitable distance in $\mathbf{x}$-space and $\langle\cdot\rangle$ indicates average over time and realizations. The mean distance d is in general a nonnegative quantity which should vanish in the synchronized state. Figure 2 (full line) displays numerical results for d as a function of ϵ in an ensemble of $N = 10^3$ logistic maps coupled as in the example considered in Figure 1. For each value of ϵ, the initial condition was prepared letting the elements evolve independently of each other during 10^3 time steps and starting from random states, but governed by the map $F(x)$. In such a way, the elements became distributed according to the invariant measure defined by $F(x)$. Then, coupling was switched on, and the interacting ensemble was left to evolve for 10^4 steps. The mean distance was calculated by averaging over the subsequent 10^2 steps. Additionally, d was averaged over 10^2 realizations of the whole process.

Surprisingly enough, it is observed that d does *not* vanish in the periodicity windows where synchronization is supposed to be stable (*cf.* Fig. 1). Furthermore, for larger coupling intensities, the point at which the mean distance reaches $d = 0$, $\epsilon \approx 0.33$, is well beyond ϵ_0. These facts can in principle be ascribed to two effects. In the first place, it could be that 10^4 steps are insufficient to reach the synchronized state from certain initial conditions. In fact, very long transients ($\sim 10^6$ steps) have recently been reported for selected values of the relevant parameters in globally coupled chaotic maps [12]. Secondly, some of the chosen initial conditions could not belong to the attraction basin of the synchronized state, their orbits converging to other attractors. In this case, the system of coupled maps would exhibit multistability properties.

In order to test these possibilities, the orbits of some selected initial conditions within the largest periodicity window ($\epsilon = 0.14$), and for coupling intensities just above the critical value ϵ_0 ($\epsilon = 0.3$) have been analyzed in detail up to much longer times ($\sim 10^7$ steps). It turns out that both situations can occur. In the periodicity window the orbits are apparently chaotic. However, in all the realizations it was observed that for sufficiently long times (10^6 to 10^7 steps) the ensemble is finally attracted to the synchronized state. In this case, thus, the fact that the mean distance in Figure 2 does not vanish within the periodicity window is due to an artifact of the numerical procedure.

On the other hand, for $\epsilon = 0.3$ it is found that the system converges typically to a state where the ensemble separates into two clusters, each of them moving in a period-2 orbit. This two-cluster regime corresponds actually to a multitude of states, since it happens that the number of elements in each cluster can vary between realizations – though it is usually near $N/2$. As a matter of fact, the existence of period-2 two-cluster states for the ensemble of coupled logistic maps can be analytically proven, by studying the solutions $x_1, ..., x_4$ to the following equations:

$$\begin{aligned} x_1 &= (1-\epsilon) f_1(x_2) + \epsilon[p f_2(x_2) + (1-p) f_2(x_4)] \\ x_2 &= (1-\epsilon) f_1(x_1) + \epsilon[p f_2(x_1) + (1-p) f_2(x_3)] \\ x_3 &= (1-\epsilon) f_1(x_4) + \epsilon[p f_2(x_2) + (1-p) f_2(x_4)] \\ x_4 &= (1-\epsilon) f_1(x_3) + \epsilon[p f_2(x_1) + (1-p) f_2(x_3)]. \end{aligned} \qquad (8)$$

Here, x_1 and x_2 are the successive states of a cluster with pN elements, and x_3 and x_4 are the states of the other cluster, with the remaining $(1-p)N$ elements. For $p = 1/2$, for instance, these equations can be explicitly solved:

$$x_{1,2} = x_{4,3} = \frac{1}{2}\left[1 + \frac{1}{(1-\epsilon)r_1}\right] \pm \frac{1}{2}\sqrt{\left[1 + \frac{1}{(1-\epsilon)r_1}\right]\left[1 - \frac{2}{r} - \frac{1}{(1-\epsilon)r_1}\right]}. \qquad (9)$$

For the values of r_1 and r_2 considered above, this solution exists for $\epsilon \lesssim 0.4$. The stability of the two-cluster states observed in the simulations has been confirmed numerically, by applying small random perturbations to the individual elements.

Consequently, for certain values of the coupling intensity the system is multistable. The synchronization state thus competes with other stable states as an attractor of the ensemble. This can be illustrated by new measurements of the mean distance d between elements, from different initial conditions. Now the initial condition is prepared by considering first a single element $x(t)$ governed by the map $F(x)$. This element is left to evolve for 10^3 steps from a random initial condition, such that its final state x_{F} belongs to the attractor of the map. Then, the initial states of the elements in the ensemble are chosen

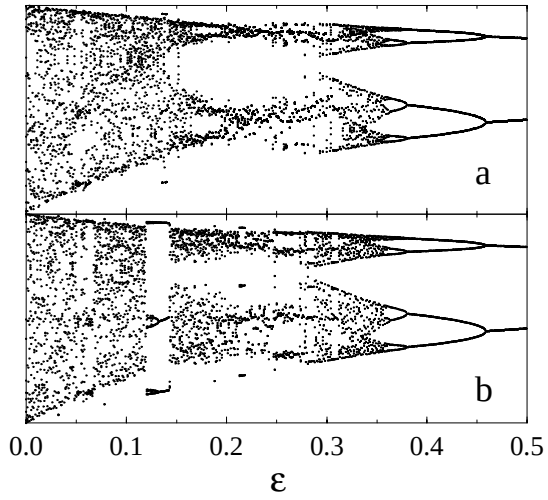

Fig. 3. Bifuraction diagram of a single element in an ensemble of 10^3 coupled logistic maps, as a function of the coupling intensity ϵ. (a) Initial conditions distributed according the invariant measure of $F(x)$. (b) Clustered initial conditions.

with uniform probability in the interval $(x_{\rm F} - \delta, x_{\rm F} + \delta)$ with $\delta = 10^{-3}$. This clustered initial condition should favor the convergence to the synchronized state. Indeed, the dashed line in Figure 2 shows that the mean distance vanishes now in the periodicity windows and for $\epsilon > \epsilon_0$, as expected.

Multistability implies that the present system is nonergodic. In particular, the definition of an order parameter for characterizing the transition to synchronization should not mix averages over time and over realizations, since they are not equivalent. In this sense, the mean distance d of equation (7) is not a proper order parameter. Moreover, there is generally no well-defined invariant measure associated with the system. A suitable illustration of this fact is provided by the bifurcation diagrams of a single element in the ensemble calculated using the two kinds of initial conditions considered above (Fig. 3). Differences in the distribution of states are apparent for $\epsilon < \epsilon_0$.

In order to test whether these results are characteristic for other choices of the individual and ensemble dynamics, the case of the (two-dimensional) Hénon map [9],

$$\begin{aligned}[x(t+1), y(t+1)] &= \mathbf{f}[x(t), y(t)] \\ &= [y(t) + 1 - ax(t)^2, bx(t)], \quad (10)\end{aligned}$$

has also been studied. For $a = a_1 = 1.4$ and $b = 0.3$ this map is well-known to exhibit chaotic behavior. If introduced in the usual globally coupled model (1), the synchronization threshold is at $\epsilon_0 \approx 0.32$. Meanwhile, for $a = a_2 = 0.3$ and the same value of b the Hénon map has a fixed point at $(x, y) = (1, 0.3)$, so that a globally coupled ensemble of such maps would synchronize for any $\epsilon > 0$. Taking now the functions $\mathbf{f}_1$ and $\mathbf{f}_2$ in equation (2) as the Hénon map with the above quoted values a_1 and a_2 of the nonlinear parameter a respectively, numerical simulations show that the same features observed for the case of the logistic maps occur here. Namely, the critical coupling intensity drops to $\epsilon_0 \approx 0.29$, wide stability windows are found for $\epsilon < \epsilon_0$, and nonsynchronized stable states – typically, clustered states with periodic orbits – exist well beyond ϵ_0. In this case, in fact, this kind of states can be observed up to $\epsilon \approx 0.5$.

It is therefore reasonable to conjecture that the following three properties are typical for globally coupled maps where the individual dynamics, governed by $\mathbf{f}_1(\mathbf{x})$, is chaotic, and the ensemble dynamics, governed by $\mathbf{f}_2(\mathbf{x})$, is periodic. (i) As a consequence of the competition between the two dynamical regimes, the critical coupling intensity from which the synchronized state is always stable decreases with respect to the case where both regimes are chaotic, *i.e.* equation (1) with $\mathbf{f} \equiv \mathbf{f}_1$. (ii) Below such critical point, a (probably infinite) set of finite intervals exists where synchronization is stable. These intervals correspond to the periodicity windows of the map $\mathbf{F}(\mathbf{x}) = (1-\epsilon)\mathbf{f}_1(\mathbf{x}) + \epsilon\mathbf{f}_2(\mathbf{x})$, which governs the dynamics of the synchronized state. (iii) In wide ranges of coupling intensities, including zones where synchronization is stable, the system displays multistability. States formed by clusters with periodic orbits are observed, and can be analytically predicted. In such zones, thus, not all the initial conditions evolve towards synchronization.

Finally, it is worthwhile to consider the extension of the present model to the case of time-continuous systems. Global coupling in an ensemble of elements whose individual dynamics is governed by the set of differential equations $\dot{\mathbf{x}} = \mathbf{f}(\mathbf{x})$ is usually introduced as [13]

$$\dot{\mathbf{x}}_i = \mathbf{f}(\mathbf{x}_i) + \epsilon(\bar{\mathbf{x}} - \mathbf{x}_i). \quad (11)$$

In this so-called vector coupling, $\bar{\mathbf{x}} = N^{-1}\sum_j \mathbf{x}_j$ and ϵ is again the coupling intensity. Synchronization is stable for $\epsilon > \lambda$, where λ is the largest Lyapunov exponent of the individual dynamics. For this model, unfortunately, it is not at all evident how to introduce a synchronized dynamics different from the individual evolution. This is however not the case in the generalization of vector coupling proposed in [11], where coupling between time-continuous systems has been introduced as

$$\dot{\mathbf{x}}_i = \mathbf{f}(\mathbf{x}_i) + \epsilon\hat{A}(\bar{\mathbf{x}} - \mathbf{x}_i) + \epsilon'[\mathbf{f}(\bar{\mathbf{x}}) - \mathbf{f}(\mathbf{x}_i)]. \quad (12)$$

Here, ϵ and ϵ' measure coupling, whereas $\hat{A}$ is a matrix whose eigenvalues are positive or have positive real parts. Vector coupling is recovered for $\epsilon' = 0$ and $\hat{A} = \hat{I}$, the identity matrix. It can be analytically shown [11] that, for $\epsilon' = 1$, the synchronized state is in this case *globally* stable. Equation (12) can be immediately generalized to introduce a prescribed synchronized dynamics, as

$$\dot{\mathbf{x}}_i = \mathbf{f}_1(\mathbf{x}_i) + \epsilon\hat{A}(\bar{\mathbf{x}} - \mathbf{x}_i) + \epsilon'[\mathbf{f}_2(\bar{\mathbf{x}}) - \mathbf{f}_1(\mathbf{x}_i)]. \quad (13)$$

If the ensemble is synchronized, its trajectory is governed by $\dot{\mathbf{x}} = \mathbf{F}(\mathbf{x}) = (1-\epsilon')\mathbf{f}_1(\mathbf{x}) + \epsilon'\mathbf{f}_2(\mathbf{x})$, in complete correspondence with (3). For $\epsilon' = 1$ the synchronized evolution

is fully defined by $\mathbf{f}_2$, and it can be proven that such state is globally stable. The details of the transition to synchronization in this time-continuous case deserve a separate presentation.

References

1. N. Khrustova, G. Veser, A.S. Mikhailov, R. Imbihl, Phys. Rev. Lett. **75**, 3564 (1995).
2. D. Domínguez, H.A. Cerdeira, Phys. Rev. Lett. **71**, 3359 (1993); Phys. Rev. B **52**, 513 (1995).
3. H. Sompolinsky, D. Golomb, D. Kleinfeld, Phys. Rev. A **43**, 6990 (1991); D. Golomb, D. Hansel, B. Shraiman, H. Sompolinsky, Phys. Rev. A **45**, 3516 (1992); H.D.I. Abarbanel, M.I. Rabinovich, A. Selverston, M.V. Bazhenov, R. Huerta, M.M. Sushchik, L.L. Rubchinskii, Usp. Fiz. Nauk. **166**, 363 (1996) [Phys. Usp. **39**, 337 (1996)]; D.H. Zanette, A.S. Mikhailov, Phys. Rev. E **58**, 872 (1998).
4. S.H. Strogatz, I. Stewart, Sci. Am. **269**, 102 (1993); S.H. Strogatz, R.E. Mirollo, P.C. Matthews, Phys. Rev. Lett. **68**, 2730 (1992); K. Kaneko, Physica D **75**, 328 (1994).
5. Y. Kuramoto, *Chemical Oscillations, Waves, and Turbulence* (Springer, Berlin, 1984); K. Kaneko, *Theory and Applications of Coupled Map Lattices* (Wiley, Chichester, 1993).
6. K. Kaneko, Prog. Theor. Phys. **72**, 480 (1984); Physica D **41**, 137 (1990).
7. H. Haken, *Principles of Brain Functioning* (Springer, Berlin, 1996).
8. G. Theraulaz, E. Bonabeau, J. Theor. Biol. **177**, 381 (1995).
9. K.T. Alligood, T.D. Sauer, J.A. Yorke, *Chaos: an Introduction to Dynamical Systems* (Springer, New York, 1997).
10. In order to avoid spurious numerical effects, in the simulations $r_1 = 4 - \Delta$ with $\Delta = 10^{-6}$. The dynamical behavior for this value of r_1 is essentially the same as for $r_1 = 4$.
11. D.H. Zanette, A.S. Mikhailov, Phys. Rev. E **57**, 276 (1998).
12. S.C. Manrubia, A.S. Mikhailov, *Very long transients in globally coupled maps* (unpublished).
13. H. Fujisaka, T. Yamada, Prog. Theor. Phys. **69**, 32 (1983); J.F. Heagy, T.L. Carrol, L.M. Pecora, Phys. Rev. E **50**, 874 (1994).